

## Controlled preparation of wet granular media reveals limits to lizard burial ability

This content has been downloaded from IOPscience. Please scroll down to see the full text.

2015 Phys. Biol. 12 046009

(<http://iopscience.iop.org/1478-3975/12/4/046009>)

View [the table of contents for this issue](#), or go to the [journal homepage](#) for more

### Download details:

This content was downloaded by: dgoldman

IP Address: 130.207.140.49

This content was downloaded on 02/07/2015 at 13:37

Please note that [terms and conditions apply](#).

# Physical Biology



## PAPER

# Controlled preparation of wet granular media reveals limits to lizard burial ability

### OPEN ACCESS

#### RECEIVED

19 December 2014

#### REVISED

16 April 2015

#### ACCEPTED FOR PUBLICATION

5 May 2015

#### PUBLISHED

25 June 2015

Sarah S Sharpe, Robyn Kuckuk and Daniel I Goldman

School of Physics, Georgia Institute of Technology, USA

E-mail: [daniel.goldman@physics.gatech.edu](mailto:daniel.goldman@physics.gatech.edu)

**Keywords:** biomechanics, granular media, locomotion

Supplementary material for this article is available [online](#)

Content from this work may be used under the terms of the [Creative Commons Attribution 3.0 licence](#).

Any further distribution of this work must maintain attribution to the author(s) and the title of the work, journal citation and DOI.



## Abstract

Many animals move within ground composed of granular media (GM); the resistive properties of such substrates can depend on water content and compaction, but little is known about how such parameters affect locomotion or the physics of drag and penetration. Using apparatus to control compaction of GM, our recent studies of movement in dry GM have revealed locomotion strategies of *specialized* dry-sand-swimming reptiles. However, these animals represent a small fraction of the diversity and presumed burial strategies of fossorial reptilian fauna. Here we develop a system to create states of wet GM of varying moisture content and compaction in quantities sufficient to study the burial and subsurface locomotion of the Ocellated skink (*C. ocellatus*), a generalist lizard. X-ray imaging revealed that in wet and dry GM the lizard slowly buried ( $\approx 30$  s) propagating a wave from head to tail, while moving in a start-stop motion. During forward movement, the head oscillated, and the forelimb on the convex side of the body propelled the animal. Although body kinematics and ‘slip’ were similar in both substrates, the burial depth was smaller in wet GM. Penetration and drag force experiments on smooth cylinders revealed that wet GM was  $\approx 4\times$  more resistive than dry GM. In total, our measurements indicate that while the rheology of the dry and wet GM differ substantially, the lizard’s burial motor pattern is conserved across substrates, while its burial depth is largely constrained by environmental resistance.

## 1. Introduction

A diversity of animals live on and within granular media (GM), materials that can display solid and fluid-like features. Dry GM such as that found in sandy deserts, are collections of particles that interact through dissipative, repulsive contact forces [1]. Using laboratory controlled substrates, recent studies (including those from our group) have investigated locomotion on dry GM; these include subsurface sand-swimming of a lizard and snake [2–4], and above-ground sidewinding snakes [5], crawling turtles [6], and running lizards [7–9]. Theoretical, computational and robotic models have helped elucidate how animals interact with the surrounding GM to generate successful forward locomotion [10–15].

Critical to these studies of movement in dry GM has been the development of apparatus (e.g. air fluidized bed trackways) that can create laboratory

versions of the environment where parameters, like compaction and grain size, can be systematically varied, resistive forces can be measured, and animal studies can be compared with models that incorporate the same substrate properties. The combined approach of experiment, modeling and substrate control has been particularly successful in developing an understanding of how the sandfish lizard *Scincus scincus* swims within dry GM by propagating a wave of curvature down its body, thereby propelling itself through a ‘frictional fluid’ (for a review see [16]). The sandfish is a dry sand specialist having adaptations which include a shovel-shaped snout, fringed toes, and ventral breathing which enable it to move effectively in dry GM.

Wet GM make up an even greater proportion [17] of terrestrial substrates, occurring in rainforest soils, coastal regions, and agricultural lands. The addition of small amounts of water to dry GM can have large

effects on the rheological properties of these substrates [18–20]. Despite the myriad of animals that walk, run, and burrow within wet terrestrial soils, few studies have explored these locomotion strategies [21–23] and even fewer animal studies have systematically varied water content and/or compaction [24] of the substrate. We note that the rheology of such unsaturated wet substrates differs from the fully saturated substrates that have been recently used to challenge other organisms, like razor clams [25] and sand lance fish [26].

Soil water content fraction can vary with factors such as geographical location, weather conditions, time of day, or depth beneath the surface. Water induces cohesion between sand grains due to the surface tension of the fluid and capillary effects [19]. This increased cohesion results in an increased angle of stability for a granular pile, such that sandcastle structures and tunnels can be formed [19, 28], and can influence mechanical properties such as shear strength [29]. As water content increases, wet GM is usually grouped into four states: pendular—in which liquid bridges form between particle contacts; funicular—where the liquid fills the pore-space spanning multiple particles but some air-filled voids remain; capillary—where all pores are filled with liquid; and the slurry state—in which particles are completely immersed in the liquid and no capillary action occurs at the surface [18, 19]. The top layer of soil found on the majority of terrestrial surfaces are in the pendular or funicular state [17].

In a review of the physics of wet GM, Mitarai [19] stressed the importance of ‘careful preparation’ of laboratory versions of wet GM to obtain reproducible results, and mentioned that compacting the wet media in a different way could generate different mechanical responses. GM compaction is characterized by the volume fraction,  $\phi$ , defined as the ratio of the volume of dry GM to the volume of the occupied space [1]. For dry granular substrates in nature,  $\phi$  can range from 0.55 to 0.63 [30]. The compaction can be controlled in the laboratory setting by using an air-fluidized bed [13, 31] in which a combination of air-flow and shaking is used to generate different  $\phi$  states. A 4% increase in  $\phi$  can increase resistance forces by 50% [2]. Wet GM can exhibit a larger range in  $\phi$  than dry GM; lower  $\phi$  states can be achieved in wet GM by the stabilizing effects of the liquid bridges [19]. However, in wet GM experiments, compaction is typically not reported or controlled.

Currently, there is no well-established technique to create repeatable, homogeneous preparations of wet GM with controllable compaction and wetness. The techniques that have been used previously include: (1) mixing the liquid and dry media, followed by slow pouring into a container [32]; (2) vigorous shaking of the liquid-sand preparation to homogeneously distribute the water [18, 29]; (3) constructing thin (2.5–5 mm thick) layers of sand and using a

fine jet to spray a known quantity of water onto each layer before another is added [33]; (4) imbibition (a wetting process) in which water is allowed to percolate through the media [34]; (5) use of a humidifier [35] to introduce water into the substrate; and (5) drainage (a drying process) [34]. Studies that have attempted to control or alter the compaction do so by using a ram [36] or by tapping the material [18, 35, 37] to achieve higher  $\phi$  states. While these methods can achieve homogeneity for high  $\phi$  states, either these methods do not produce low  $\phi$  preparations or, if they do, in our experience these preparations may contain large voids which vary in size and location from trial to trial.

An example of an animal that successfully [27, 38] contends with GM of different water contents is the Ocellated skink (*Chalcides ocellatus*), a habitat generalist lizard found in coastal regions and near vegetation where moist sand is common (figure 1) [27]. The Ocellated skink has a slender body with relatively reduced limbs [39] that lack toe fringes and, like the specialist sand-swimming sandfish lizard, has a wedge-shaped head. Ocellated skinks are commonly found near vegetation and ‘harder’ soil whereas the sandfish is found farther from vegetation on the dry, aeolian sands of the dunes. Field observations have shown that the Ocellated skink spends most of its time near cover and will bury into granular substrates to seek refuge from heat and predators [40]. We note that Ocellated skinks co-exist with the sandfish lizards in the sand dunes of North Sinai, Egypt [40]. However, within this environment the Ocellated skink occupies a different micro-habitat. Thus for these two lizards of the family Scincidae that occupy the same regions of northern Africa and the middle east, it is interesting to contemplate how the generalist Ocellated skink’s burial pattern compares to the specialist sandfish skink in dry GM and how the Ocellated skink’s burial pattern changes with substrate properties.

In this paper we present a new technique which uses a sieve apparatus to deposit mixed wet GM into a container, resulting in an initially loosely packed state without large voids; we then utilize additional shaking to achieve a desired compaction. Using this technique in combination with x-ray imaging allows us to systematically study how substrate properties affect burial mechanics and performance of the Ocellated skink, and also enables characterization of substrate resistance. We will show that, despite common ancestry and an overlap of ranges, the Ocellated skink does not swim like the sand-specialist sandfish lizard (the only other sand-swimming lizard studied in detail to date [2, 3, 15]) which swims at relatively high forward speeds ( $\approx 10 \text{ cm s}^{-1}$  or  $0.9 \text{ SVL s}^{-1}$ ) using large amplitude body undulations while its limbs remain close to its body. Instead we will show that the generalist Ocellated skink uses a more complex burial pattern involving body undulation, head oscillation and limb use. The locomotion pattern is similar across substrate conditions, and drag force measurements indicate that

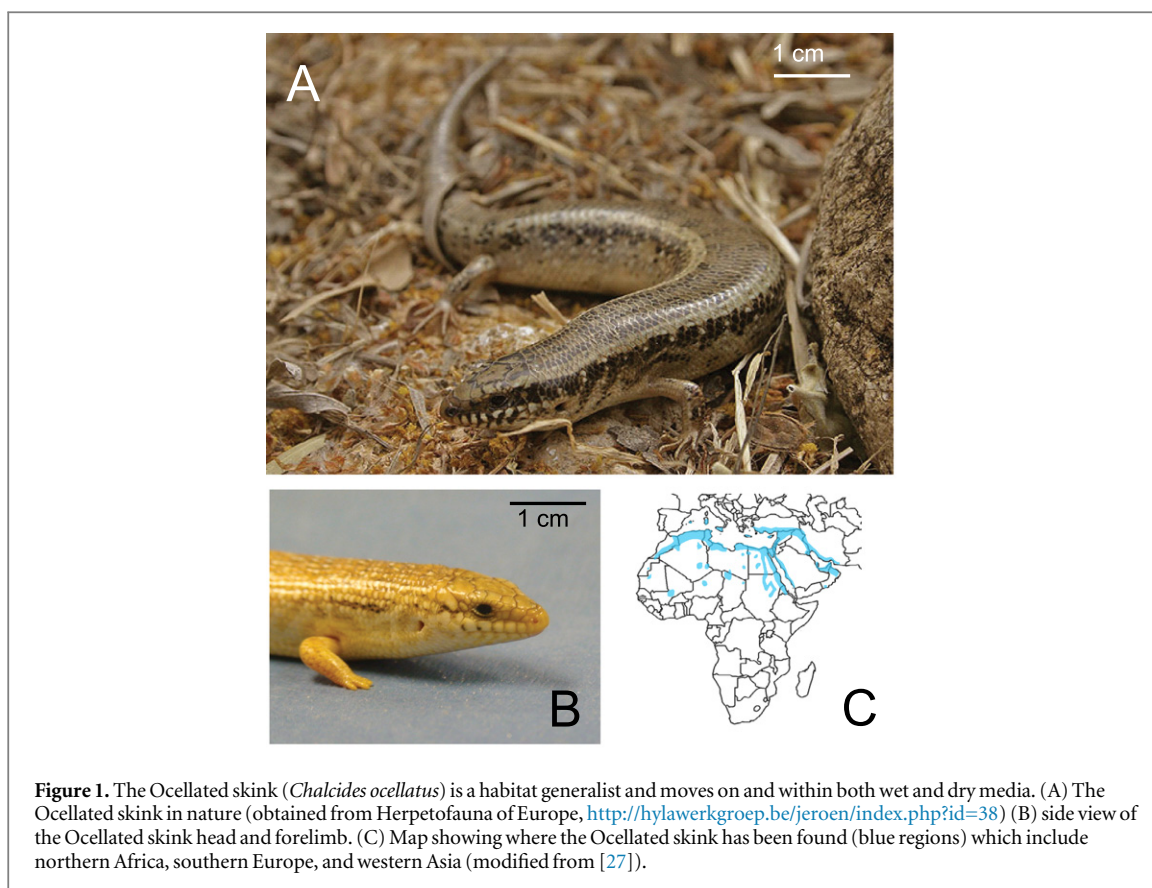


**Figure 1.** The Ocellated skink (*Chalcides ocellatus*) is a habitat generalist and moves on and within both wet and dry media. (A) The Ocellated skink in nature (obtained from Herpetofauna of Europe, <http://hylawerkgroep.be/jeroen/index.php?id=38>) (B) side view of the Ocellated skink head and forelimb. (C) Map showing where the Ocellated skink has been found (blue regions) which include northern Africa, southern Europe, and western Asia (modified from [27]).

this pattern constrains the animal to bury to depths largely limited by muscular force of body bending.

## 2. Materials and methods

### 2.1. Dry media preparation

Loosely packed (LP) dry GM preparations ( $\phi = 0.58 \pm 0.01$ ) were created using an air-fluidized bed with an area of  $22.9 \times 40.6 \text{ cm}^2$  and filled with spherical glass particles to a height of 10 cm ([2, 3]). The particles were similar in size (diameter =  $0.27 \pm 0.04 \text{ mm}$ ) and weight (density =  $2.5 \text{ g cm}^{-3}$ ) to sand found in nature. An evenly distributed air flow was forced upward through the grains; below a critical flow rate grains remained stationary, and above this flow rate the grains moved relative to each other (which is referred to as fluidization). To generate the LP states, the medium was fluidized followed by a slow decrease in flow rate to zero. Air flow was off during force measurements and animal burial trials.

### 2.2. Wet media preparation

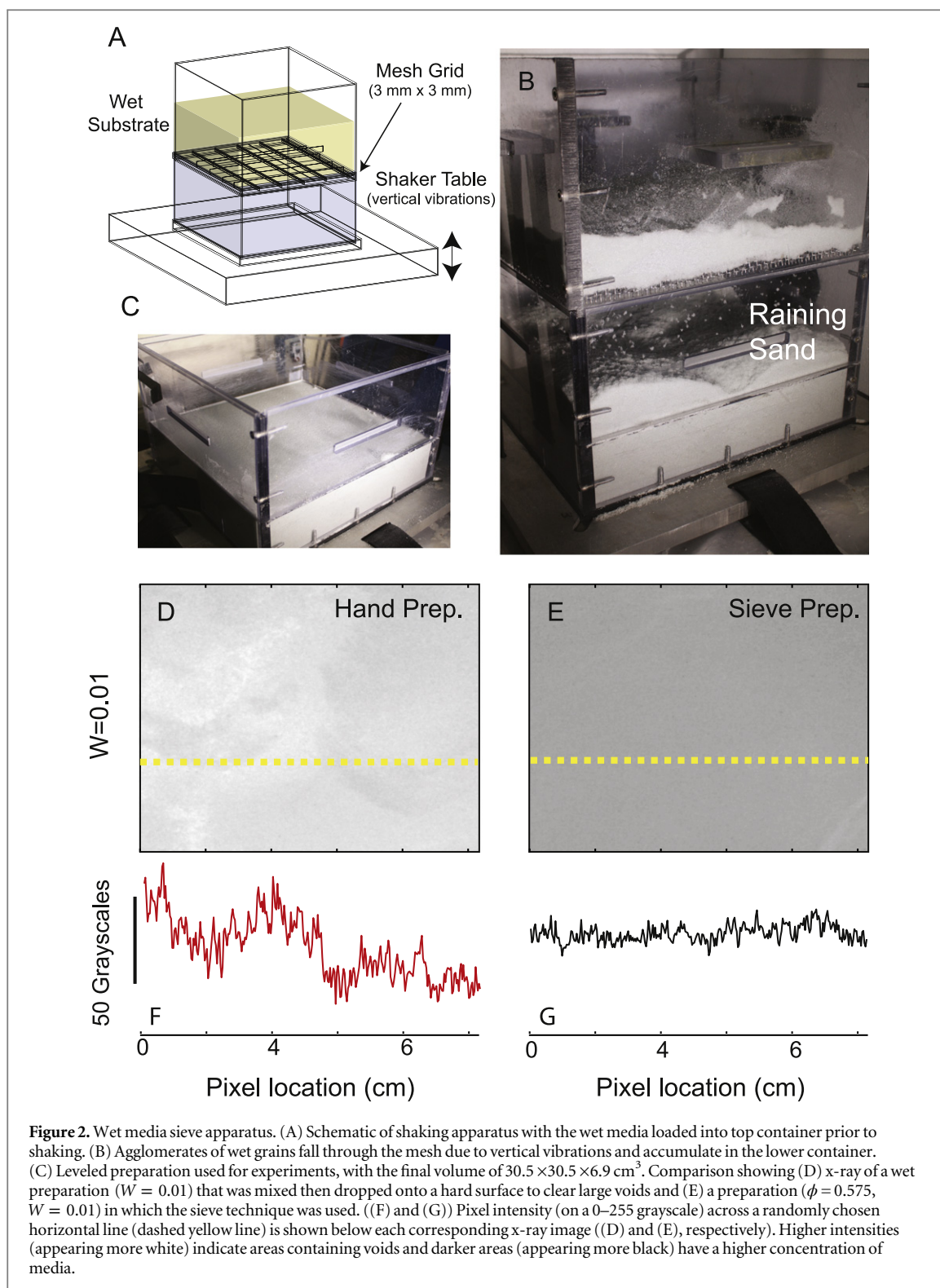
#### 2.2.1. Wet media mixture

A high-speed hand mixer (Hamilton Beach/Proctor-Silex, Southern Pines, NC) was used to combine 14 kg of dry spherical glass particles (diameter =  $0.27 \pm 0.04 \text{ mm}$ , density =  $2.5 \text{ g cm}^{-3}$ ) with 0.14, 0.42 and 0.7 kg of water, such that  $W = 0.01, 0.3,$  and  $0.05$  water content preparations were achieved, where  $W$  is defined as the ratio of the mass of the water to mass of the dry GM. The media were mixed for at least 3 min

to distribute water evenly throughout the preparation. Media preparation and experimentation took place in a room with a humidity level of  $\approx 41\%$  and temperature of  $\approx 25^\circ\text{C}$ . The wet mediums were used in experiments for only two hours after preparation to limit changes in water content due to evaporation. We characterized water loss due to evaporation by preparing  $W = 0.01, 0.03, 0.05$  mixtures and weighing the substrates periodically. The substrates were stirred once every hour. These experiments revealed that  $W$  decreased by  $0.0014 \pm 0.0003$  after two hours for all starting  $W$  preparations.

#### 2.2.2. Apparatus development

A ‘sieve’ apparatus was constructed to deposit media homogeneously into a testing container (figure 2, see SI Video 2 available at <http://stacks.iop.org/pb/12/046009/mmedia>). The sieve apparatus consisted of two polycarbonate boxes ( $30.5 \times 30.5 \times 19.5 \text{ cm}^3$ ) that were stacked vertically, a holding plate, and a vertical shaker. The top box was separated from the bottom container by a stainless steel woven mesh grid (wire diameter = 1.2 mm, opening area of  $3 \times 3 \text{ mm}^2$ ). The prepared wet media was poured into the top container of the sieve apparatus. Cohesion between grains prevented the media from falling through the mesh when the apparatus was stationary. The stacked boxes fit into a holding plate and were secured using straps which prevented relative motion between the boxes and plate during shaking (figure 2(A)). Sinusoidal vertical vibrations, with a frequency of 60 Hz and average amplitude



of 1.75 mm, were applied to the holding plate via the electromagnetic shaker (VTS, Aurora, OH). These parameters were selected due to our observations that media readily fell through the mesh when these vibration parameters were used (figure 2(B), and see SI Video 2 [stacks.iop.org/pb/12/046009/mmedia](http://stacks.iop.org/pb/12/046009/mmedia)). The shaker was controlled using custom software (LabVIEW, National Instruments, Austin, TX) and a power amplifier (Model # 7550, Techtron, Elkhart, IN). Vibrations were monitored using an accelerometer (PCB

Piezotronics, Depew, NY) that was attached to the holding plate. The software monitored the shaking and maintained the desired shaking parameters using a PID controller. Changing the amplitude and/or frequency of the vibrations changed the efficacy of inducing media deposition. Analysis of how these parameters affect the final medium compaction is beyond the scope of the present study.

Shaking ceased after the sieved material in the lower container exceeded a height of 7 cm. A slit and

groove located at  $7.06 \pm 0.16$  cm from the base in the lower box allowed a thin aluminum plate to slide into the container separating the GM into two sections. The top media above the thin plate was removed leaving a volume of wet media ( $30.5 \times 30.5 \times 6.9$  cm<sup>3</sup>) with a level surface which was used for experiments (figure 2(C)). The volume fraction,  $\phi$ , was determined by weighing the wet media. Due to the leveling technique, the volume of the space occupied remained constant across trials. The volume of the dry GM was determined from the relation  $V_{GM} = \frac{M_{wet}}{\rho_{GM}(1+W)}$ , where  $\rho_{GM}$  is the density of the GM,  $M_{wet}$  is the mass of the wet media and  $W$  is the water content. Due to the error in the volume and  $W$  measurements, we estimate a systematic error in the  $\phi$  calculation of  $\pm 0.007$ .

### 2.2.3. Technique characterization and capabilities

**Homogeneity**—we evaluated the homogeneity of a sieved wet media preparation ( $W = 0.01$ ,  $\phi = 0.575$ ) using x-ray imaging (source: OEC-9000, Radiological Imaging, Hamburg, PA, USA; detector: Varian flat panel 25250 V Csl, Palo Alto, CA, USA) (figures 2(D) and (E)). The x-ray was set to an energy of 20 mA and 60 kV. Variations within the substrate were detected by examining the pixel intensity (on a 0–255 grayscale) where higher intensities (appearing more white) indicate areas containing voids and darker areas (appearing more black) have a higher concentration of media. The sieved preparation was compared to wet media ( $W = 0.01$ ) that was mixed then compacted by ‘hand’ by dropping the media container from a height between 5 and 8 cm multiple times onto a hard surface to remove large voids. Fluctuations in the local density hand prepared states were larger ( $\approx 50$  grayscales, figures 2(D) and (F)) compared to fluctuations in the sieve preparation ( $\approx 10$  grayscales, figures 2(E) and (G)).

**Compaction**—it took at least 70 s of shaking to deposit 7 cm (in height) of media in the bottom container. The average time for all wet media ( $\approx 14$  kg) to fall through the mesh increased with wetness content ( $188.5 \pm 62.6$  s for  $W = 0.01$ ,  $287.9 \pm 84.8$  s for  $W = 0.03$ , and  $316.4 \pm 119.7$  s for  $W = 0.05$ ). The total shaking time was varied between 70 and 2250 s to achieve varying compactions.

### 2.3. Force measurements

To measure penetration resistance and drag force in wet and dry GM, a robotic arm (CRS robotics, Burlington, Ontario, Canada) with 6 degrees of freedom was used to drive a stainless steel cylindrical rod (diameter = 1.6 cm and length = 3.81 cm) through the media. A support rod (diameter = 0.63 cm) and nut (height = 0.55 cm, corner-to-corner width = 1.25 cm) were used to attach the cylindrical intruder to a force sensor (ATI industrial, Apex, NC, USA), accurate to 0.06 N, located on the robot end effector. The cylinder was submerged 3.2 cm into the GM (measured from

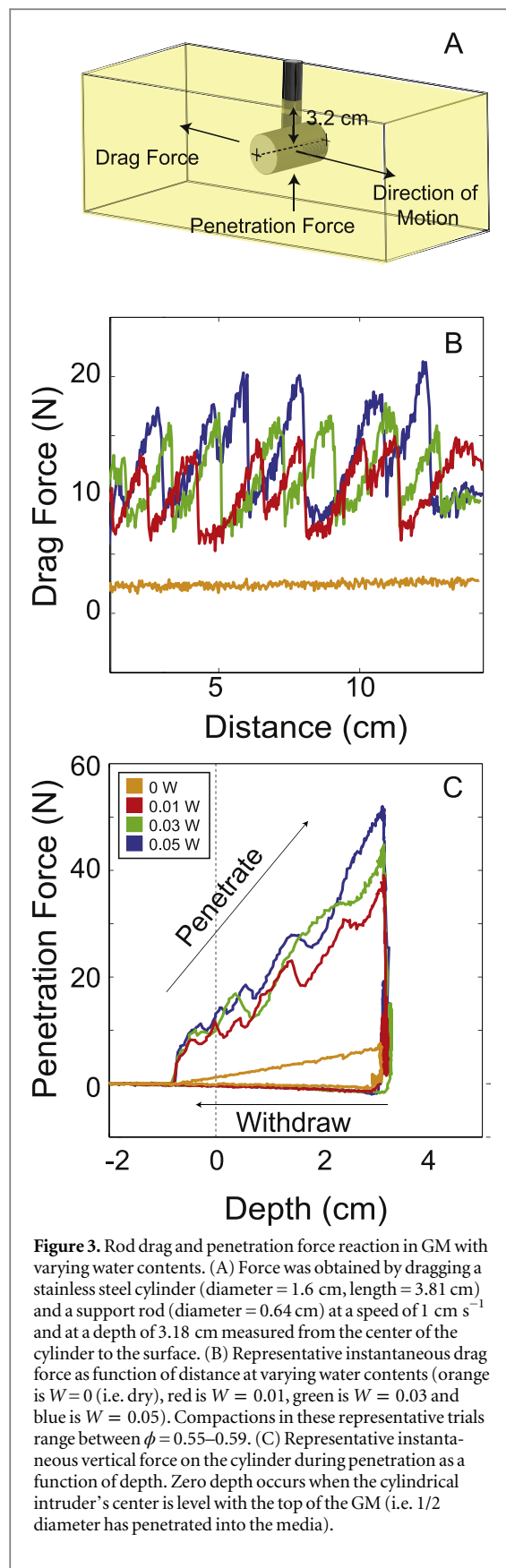
its center axis to the surface of the substrate), and the cylinder was dragged 12.7 cm with its long axis oriented perpendicular to the direction of motion (figure 3(A)). Speed during penetration and drag was  $1$  cm s<sup>-1</sup> (for intruders of this size force is insensitive to speed in dry GM below  $\approx 50$  cm s<sup>-1</sup> [2, 3] and preliminary studies indicate the same force insensitivity in wet media). The total projected area of the cylinder, submerged support rod and nut during drag was 8.4 cm<sup>2</sup>. The instantaneous force periodically fluctuated due to material fracturing that occurred during movement within the substrate (see results, figure 3(B)); consequently, the average drag force was calculated during steady state movement from the start of one oscillation to the start of another oscillation. Although we did not investigate the fluctuations in the plowed wet GM, it would be interesting to compare their dynamics to the force fluctuations observed in compact dry GM described in [31].

To quantify the average drag force as a function of depth on an intruder with the same projected area (6.1 cm<sup>2</sup>), the drag force on the support rod and nut was subtracted from the drag force of the cylinder + support rod and nut. Drag force as a function of depth was quantified in dry media ( $\phi \approx 0.58$ ) and in  $W = 0.03$  wet media ( $53.2 \leq \phi \leq 55.7$ ).

### 2.4. Ocellated skink experiments

Ocellated skinks, *Chalcides ocellatus*, (figure 1) were purchased from commercial vendors (East Bay Vivarium, Berkeley, CA, USA and Ocean Pro Aquatics, Chino Hills, CA, USA). The four animals used in this study had an average snout-vent length (SVL) of  $10.9 \pm 1.3$  cm, snout-tail length of  $18.6 \pm 3.2$  cm and mass of  $21.5 \pm 6.8$  g. The ocellated skink’s body height is  $1.3 \pm 0.2$  cm and width is  $1.8 \pm 0.3$  cm ( $N = 4$  animals). All animals were housed individually in large containers ( $21 \times 43 \times 28$  cm<sup>3</sup>) filled with moist sand to a depth of 15 cm and were provided with a water dish and moss for hiding. Ocellated skinks were given six mealworms coated in a supplemental calcium powder twice a week and allowed to eat *ad libitum*. The holding room was maintained on a 12 h:12 h light:dark cycle. All experimental procedures were conducted in accordance with the Georgia Institute of Technology IACUC protocol numbers (A08012, A11066) and Radiation Safety protocol (X-272).

We compared the burial strategy of the Ocellated skink on LP ( $\phi = 0.56 \pm 0.01$ ) wet GM ( $W = 0.03$ ) to the strategy used on LP dry GM ( $\phi = 0.58 \pm 0.01$ ). LP wet media was used because Ocellated skinks did not bury as readily into closely packed (CP) wet media. Ocellated skinks were placed on top of the media preparation inside of a 14.5 cm diameter hollow plastic cylinder resting on the surface of the substrate which induced burial at a desired location. For enhanced contrast, a minimum of 11 lead markers ( $\approx 1$  mm<sup>2</sup> each, mass  $\approx 0.01$  g) were placed on the skink’s dorsal



midline at 0.1 SVL increments and one marker was placed on each limb. Above-surface visible light video was recorded at 63 frames per second (fps) using a high speed camera (AOS Technologies AG X-PRI,

Baden Daettwil, Switzerland) to characterize general features of above surface movement such as time to burial and limb use. Top-view subsurface kinematics were recorded using an x-ray system (OEC 9000, Radiological Imaging Systems, Hamburg, PA, USA) coupled to a high speed camera (Fastcam 1024 PCI, Photron, San Diego, CA, USA) which recorded at 60 fps. The different above surface and subsurface video frame rates were set due to camera constraints. For dry GM preparations, the x-ray system was set to 85 kV at 20 mA, and for wet preparations, to 73 kV and 20 mA. Ocellated skink burial time was determined from above surface video as the time it took for the animal to submerge such that the head to vent was covered by the substrate. When the anterior portion of the animal was buried prior to the start of the above surface recording, then the time to burial was calculated as the time it takes for the above surface fraction of the SVL to submerge divided by the proportion of the SVL above surface at the beginning of the recording.

To determine angle of entry and final depth of burial in wet and dry GM, biplanar x-ray videos were acquired. The OEC-9000 x-ray system was again used to record top view images. An additional x-ray system (source: Spellman XRB502 Monoblock, Hauppauge, NY, USA; flat panel detector: Varian 25250 V Csl, Palo Alto, CA) was oriented  $90^\circ$  with respect to the top view x-ray such that side view images of the subsurface locomotion were simultaneously obtained. The flat panel detector captured images at 30 fps. The width of the wet GM container was decreased to  $\approx 17$  cm by using foam inserts. Decreasing the width was necessary to enhance contrast between the Ocellated skink and surrounding media during side view imaging. Opaque lead markers were placed on the dorsal midline, and along the animal's side closer to the ventral surface to enable visualization of the Ocellated skink in both top and side view images. 3D reconstructions were made using custom software (Matlab, Mathworks, Natick, MA, USA). Depth of burial was assessed by measuring the distance from the substrate surface to the ventral midpoint ( $\approx 0.5$ – $0.6$  SVL) along the body at the animals final resting position.

### 3. Results

#### 3.1. Penetration and drag forces in a wet substrate

Instantaneous force during drag (figure 3(B)) and penetration (figure 3(C)) revealed a large increase ( $\approx 4$  times greater) in force between dry and wet GM preparations. During penetration, force increased with depth (figure 3(C)) for both dry and wet substrates. During withdrawal, there was a slight negative force in all substrates. We attribute this negative force to the weight of material above the rod and the shearing forces that occur between the grains.

Force fluctuations occurred in wet substrates during penetration and drag which corresponded to material fracturing visible at the surface. These large force fluctuations resemble shear band formation and fracturing during drag in CP dry media [31]. The mechanism by which these bands occur in wet media has not been investigated and is beyond the scope of this work. In agreement with previous studies [2, 31], these large force fluctuations were not present during drag in LP dry media.

Average drag in  $W = 0.01$  wet media ( $\phi = 0.58$ ) was  $\approx 4$  times larger than the average drag force in dry media ( $0 W$ ,  $\phi = 0.58$ ; figure 4). The average force continued to increase as  $W$  increased from 0.01 to 0.05 (ANCOVA,  $F(5, 59) = 32.0$ ,  $P < 0.001$ ), but by a smaller amount ( $\approx 1$  N per 0.01 increase in  $W$ ). Resistance forces increased with compaction in  $W = 0.01, 0.03, 0.05$  preparations (figure 4(B), ANCOVA,  $F(5, 59) = 7.5$ ,  $P < 0.01$ ). Force changes were large with small changes in  $\phi$ ; for example, force increased by 50% in  $W = 0.03$  media from approximately 8.0 N at  $\phi = 0.53$  to 11.8 N at  $\phi = 0.58$ .

### 3.2. Ocellated skink burial in wet and dry media

After being placed on the  $W = 0.03$  wet media, Ocellated skinks took between 1 and 30 min before initiating burial. Lightly squeezing or gently tapping the animals' tails occasionally induced burial more quickly. Examples of X-ray and above surface images during Ocellated skink burial are shown in figure 5. Ocellated skinks rarely buried into substrate preparations with  $\phi > 0.58$  and so LP preparations of wet GM ( $\phi \leq 0.56$ ) were used in all experimental trials. Initiation of burial took less time in dry GM (between 1 and 15 min).

After initiation, Ocellated skink burial was slow relative to sandfish burial (see SI Video 1 available at <http://stacks.iop.org/pb/12/046009/mmedia>). Burial time was moderately smaller in dry media ( $22.9 \pm 13.4$  s) compared to wet media ( $29.4 \pm 9$  s, ANOVA,  $F(7, 36) = 4.5$ ,  $P < 0.05$ ) and differed slightly among animals tested (ANOVA,  $F(7, 36) = 3.0$ ,  $N = 4$  animals). This slow burial was in part a consequence of the start-stop locomotion strategy that the Ocellated skink used during burial (figure 6). Figures 6(C) and (D) show the movement of the 5th marker (at the 0.4 SVL location) on the Ocellated skink for a representative trial in wet and dry media, respectively, where the displacement is a measure of the total distance along the path length from the beginning of the trial. The plateaus (pink regions) indicate pauses while the green regions correspond to progression. Ocellated skinks moved for an average of 0.6 s in both wet and dry media before pausing ( $N = 4$  animals,  $n = 5-7$  trials each); histograms of the movement and stopping times are shown in figures 6(E)–(H). The average subsurface speed of the 0.4 SVL location during movement was higher in dry media ( $0.21$

$\pm 0.05$  SVL  $s^{-1}$ ;  $2.4 \pm 0.5$  cm  $s^{-1}$ ) compared to in wet media ( $0.11 \pm 0.03$  SVL  $s^{-1}$ ;  $1.1 \pm 0.2$  cm  $s^{-1}$ , T-test,  $P < 0.01$ ).

Most Ocellated skinks placed their hindlimbs near their sides prior to limb submergence (see SI Video 1 available at <http://stacks.iop.org/pb/12/046009/mmedia>). This occurred when  $0.8 \pm 0.2$  of the SVL was submerged in the media for both wet and dry substrates and across all animals tested (ANOVA,  $P > 0.05$ ). In both wet and dry media, Ocellated skinks had a curved body posture during burial resembling a serpentine curve with  $\approx 1.5$  waves along the body and the subsurface slip was low (i.e. all body locations followed a similar trajectory, figures 6(A) and (B), see SI Video 3 available at <http://stacks.iop.org/pb/12/046009/mmedia>). While the hindlimbs were placed by the animal's sides before burial, the skink continued to use its forelimbs during subsurface locomotion. Protraction and retraction of the forelimb on the convex side of the body was observed during forward progression and the forelimb on the concave side was held near the body (see SI Video 3 available at <http://stacks.iop.org/pb/12/046009/mmedia>).

The head rotated from side to side (oscillated) during forward locomotion at  $\approx 2-4$  Hz (see SI Video 3 available at <http://stacks.iop.org/pb/12/046009/mmedia>). Figure 7(A) shows the trajectory of markers along the body. The side to side motion is clearly visible in the trajectory of the snout marker (blue trajectory), while other markers follow along its mean path. There was a lower amplitude deviation in the 2nd and 3rd marker as well, indicating that the pivot point was between the 0.2 and 0.3 SVL locations. The angle of excursion about the pivot point was estimated by low pass time-filtering, the position of the snout (1st) marker, using a first order Butterworth filter and 15 Hz cut-off frequency, and comparing the vector between the filtered 1st marker position and the 4th marker position with the vector between the actual 1st marker position and 4th marker position (figure 7(B)). The maximum angle of excursion in dry media ( $7.6^\circ \pm 2.3^\circ$ ,  $n = 10$  trials,  $N = 3$  animals) was higher than the maximum angle in wet media ( $4.5^\circ \pm 1.3^\circ$ ,  $n = 9$  trials,  $N = 3$  animals; ANOVA,  $F(2, 18) = 10.3$ ,  $P < 0.01$ , figure 7(C)) and did not statistically vary across animals.

There was a substantial difference in the burrowing angle between wet and dry substrates (see SI Video 4 available at <http://stacks.iop.org/pb/12/046009/mmedia>). Ocellated skinks in dry media burrowed at an average angle relative to the horizontal surface of  $31.6^\circ \pm 8.6^\circ$ , while in wet media the angle was smaller  $8.0^\circ \pm 3.8^\circ$  (figure 8(C)). The average depth of burial in dry media ( $5.0 \pm 1.5$  cm) was over three times as large as the average depth of burial into wet media ( $1.6 \pm 0.5$  cm; figure 8(B)).

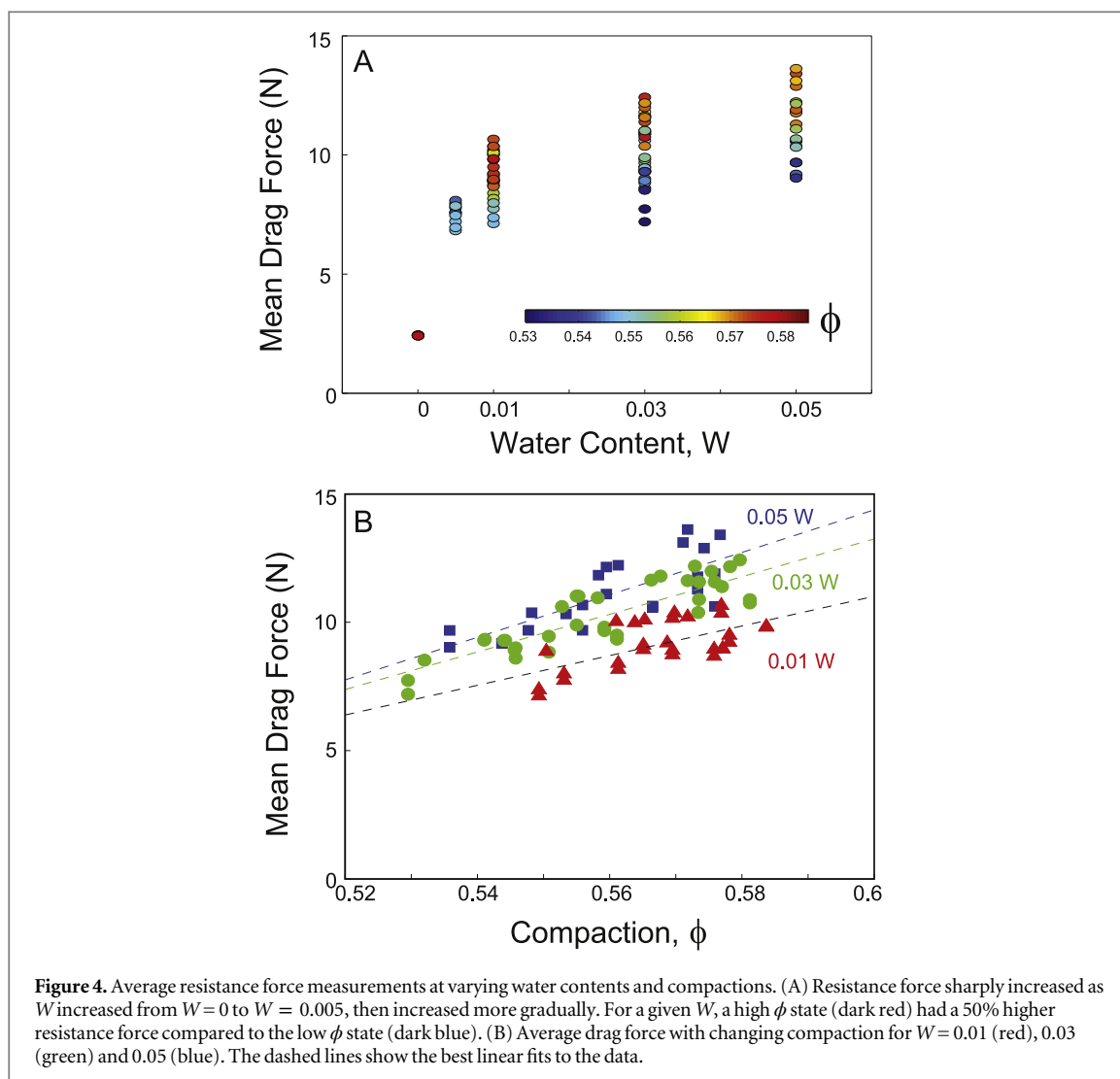


**Figure 4.** Average resistance force measurements at varying water contents and compactions. (A) Resistance force sharply increased as  $W$  increased from  $W = 0$  to  $W = 0.005$ , then increased more gradually. For a given  $W$ , a high  $\phi$  state (dark red) had a 50% higher resistance force compared to the low  $\phi$  state (dark blue). (B) Average drag force with changing compaction for  $W = 0.01$  (red), 0.03 (green) and 0.05 (blue). The dashed lines show the best linear fits to the data.

## 4. Discussion

### 4.1. Preparation of states of wet GM

The new sieving method created large homogenous preparations of wet GM (i.e. no large voids) with variable compactions. Low  $\phi$  states were achieved by stopping the vibrations soon after media deposition, while high  $\phi$  states were achieved by prolonged shaking. Depending on shaking time, compaction varied between  $\phi = 0.53$ – $0.60$ . As expected due to the stabilizing effect of liquid bridges, the minimum  $\phi$  obtained in wet media was lower than the minimum  $\phi$  achieved in dry media ( $\phi = 0.58$ ) using the air-fluidization technique. We expect that lower compactions ( $\phi < 0.53$ ) could be achieved by shaking the top container only; in our system, both the top and bottom containers were shaken simultaneously during the deposition process. Therefore, the media that was deposited into the lower container near the onset of shaking may be at a slightly higher compaction. However, we were unable to distinguish a compaction gradient within the material using x-ray imaging. Applying vertical vibrations to the top container alone

would help to remove the compaction gradient, if it exists, and create an overall lower  $\phi$ . The highest compaction achieved ( $\approx 0.6$ ) occurred after 40 min of shaking. For all wet media preparations, the compaction of the media increased logarithmically with shaking time. Fiscina *et al* [37] found that  $\phi$  as large as 0.62 could be achieved in water–GM mixtures. Since we did not observe an asymptote in compaction with increased shaking time, we expect that larger compaction preparations are possible using our setup for shaking time  $> 40$  min. However, for animal experimentation this might be impractical since the media preparation time would be inconvenient.

### 4.2. Resistance forces

We found that penetration and drag resistance forces increased with wetness (for example, drag forces increased 400% from dry to  $W = 0.01$  media) and with compaction (drag forces increased 50% between LP and CP in  $W = 0.03$  media). These results emphasize the importance of controlling and reporting both  $W$  and  $\phi$  when performing animal and robotic locomotion studies in wet GM since changes

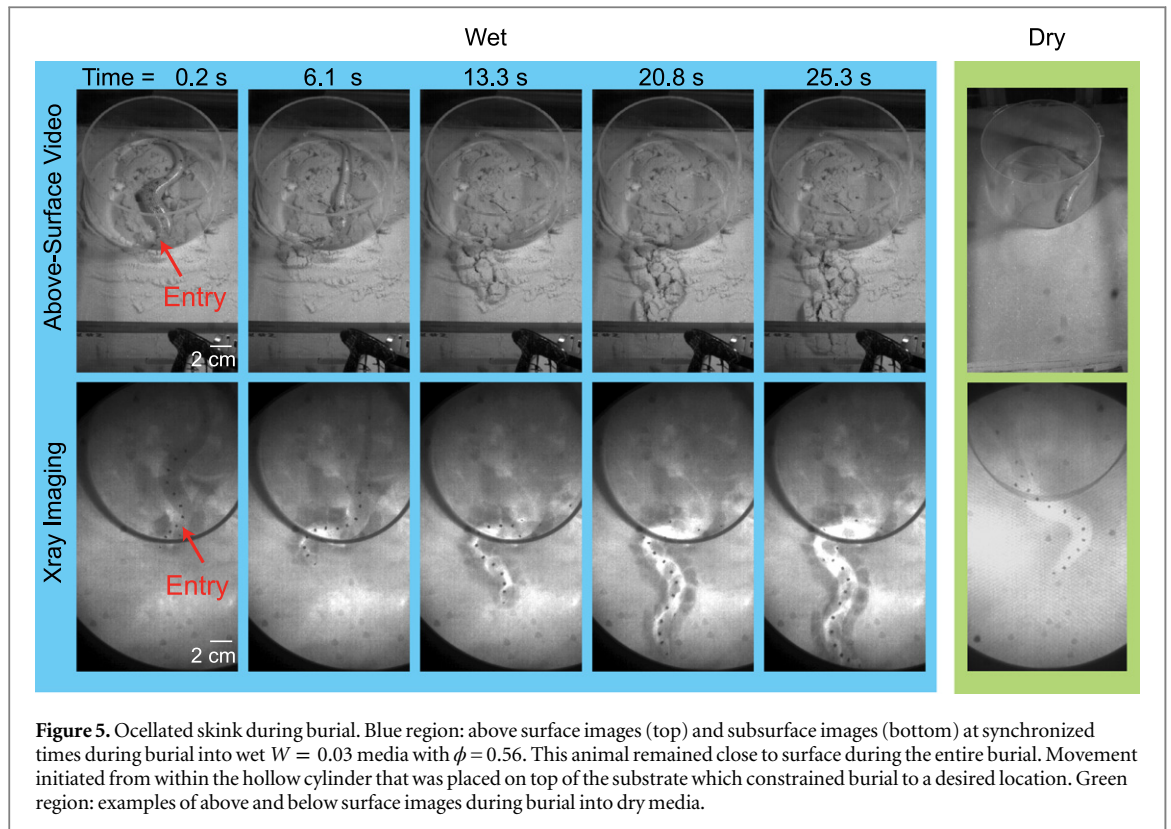


**Figure 5.** Ocellated skink during burial. Blue region: above surface images (top) and subsurface images (bottom) at synchronized times during burial into wet  $W = 0.03$  media with  $\phi = 0.56$ . This animal remained close to surface during the entire burial. Movement initiated from within the hollow cylinder that was placed on top of the substrate which constrained burial to a desired location. Green region: examples of above and below surface images during burial into dry media.

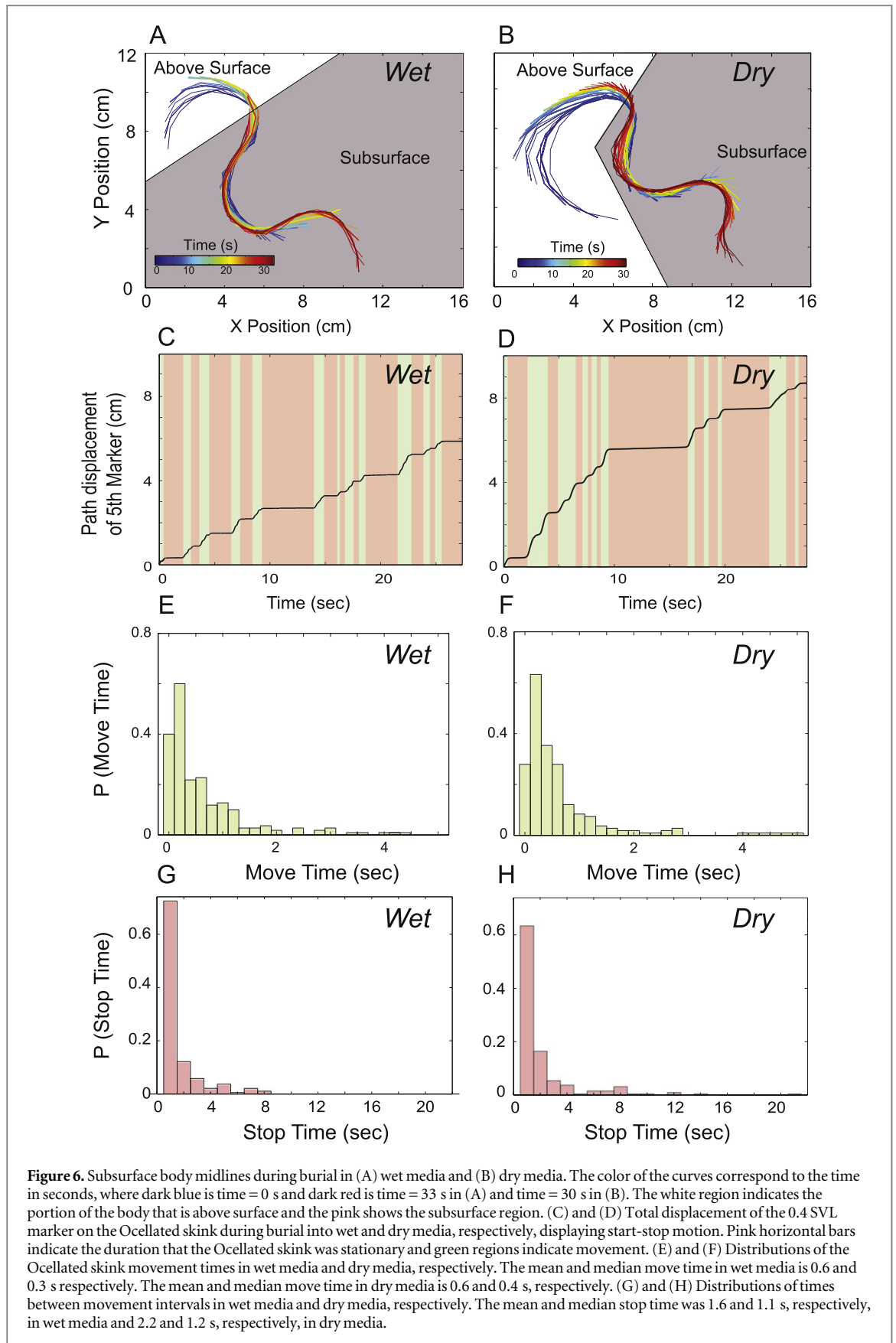
in resistance force could influence locomotion strategy and/or kinematics. The average drag force in the wet media preparations displayed larger standard deviations among different trials compared to the dry force measurements. We attribute this deviation to the large force fluctuations during drag in wet media. Although we measured mean force over one fluctuation period, changes in the fluctuations (such as the frequency and/or minima) may have skewed mean values (see figure 3(B)). A more in-depth study which examines these force fluctuations with water content could lead to more consistent results and reveal principles of the response of wet GM to localized intrusions.

In dry GM at the speeds the animal operates (a few  $\text{cm s}^{-1}$ ) drag forces are insensitive to drag speed [2, 41]. We found similar results in slightly wet GM ( $W < 0.1$ ): rod drag experiments at different speeds (1, 5, and  $10 \text{ cm s}^{-1}$ ) also revealed that force was insensitive to speed (see supplementary material, figure S1 [stacks.iop.org/pb/12/046009/mmedia](http://stacks.iop.org/pb/12/046009/mmedia)). We note that these experiments were conducted in wet sand preparations that were created via hand-mixing and therefore compaction was not controlled. However, since compaction does not increase speed sensitivity in dry GM, we expect that for a given  $W$  and compaction, drag forces will remain insensitive to speed. However, we suggest that future studies should test this hypothesis.

We comment briefly on the applicability of our rod drag experiments to infer properties of drag on the animal's body. Although the stainless steel cylindrical intruder used to estimate resistance force has different

properties than the Ocellated skink's body, we expect that for fixed body properties the trend of increasing forces with water content can be extended to the forces experienced by the lizard. The diameter of the rod is comparable to the body diameter of the Ocellated skink. Furthermore, we have shown that in dry material, force scales with the projected area of the intruder. While the Ocellated skink's skin-particle friction ( $0.15 \pm 0.02$  on the ventral surface in the forward direction and  $0.13 \pm 0.01$  on the dorsal surface in the forward direction, see [4, 42] for discussion of the technique) is about half that of the rod-particle friction, normal drag force is independent of the friction of the rod. The rod was moved in the GM with its long axis normal to the direction of travel in order to maximize normal drag force and minimize tangential force which scales with friction. Finally, we expect water adhesion properties to be similar enough between the rod and Ocellated skink's body such that force characteristics are the same. Skin wettability for lizards that inhabit arid regions have a range of adhesion properties but all tend to have water contact angle  $< 90^\circ$  and therefore are hydrophilic [43]. The stainless steel is also hydrophilic. Future investigation of the skin properties of the Ocellated skink's skin is needed to better determine how its body properties affect resistance forces during movement.

In dry GM, a granular resistive force theory (RFT) was developed to understand the continuous serpentine motion of the sandfish and shovel-nosed snake moving subsurface in dry [4]. This GM theoretical model, which employs the use of empirically



measured normal and tangential forces on a small rod moving through GM, assumes steady-state motion of the animals. However, because the Ocellated skink employs a start-start motion we did not attempt to

apply RFT to understand the forces imparted on the skink's body during movement through dry GM. Future developments of RFT in dry GM should account for such transient phenomena (which are

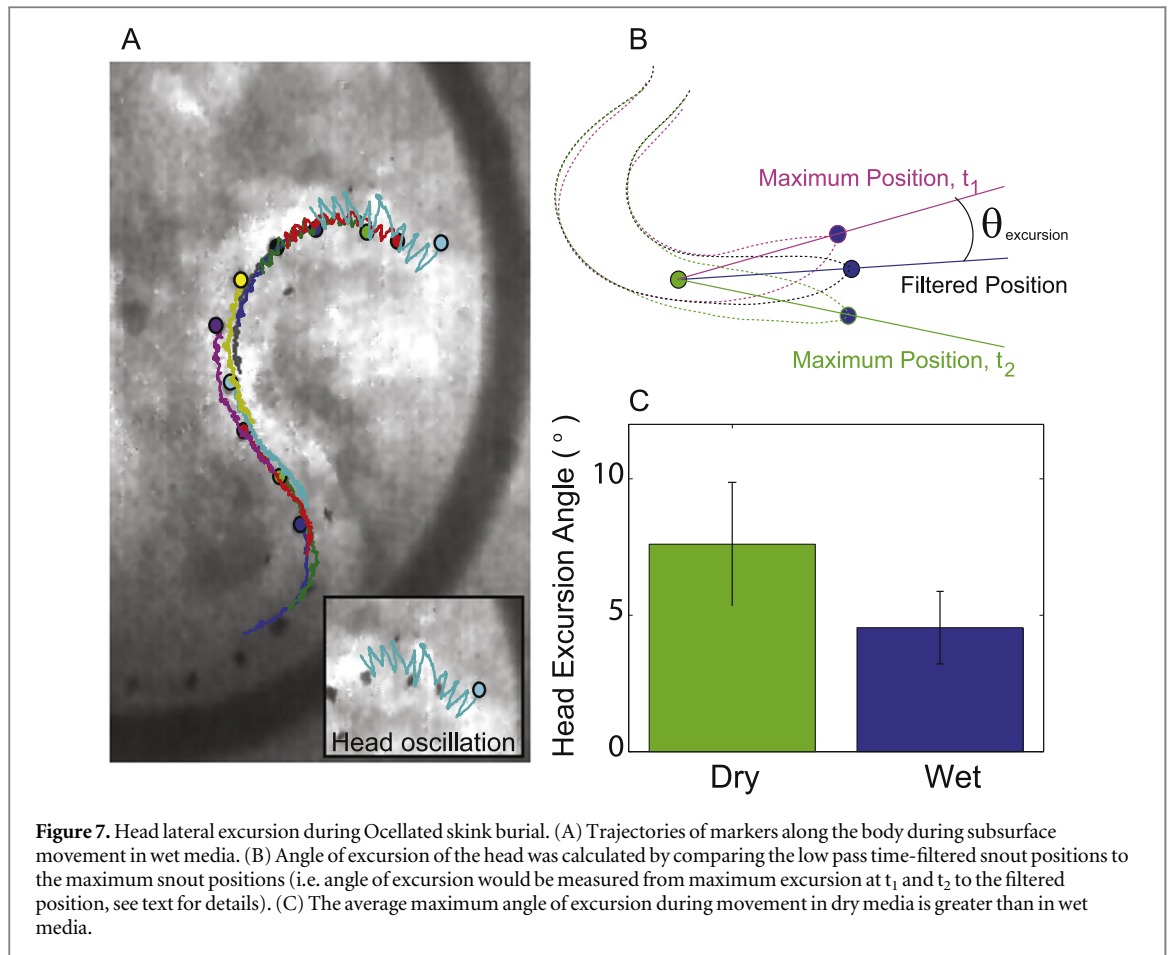


**Figure 7.** Head lateral excursion during Ocellated skink burial. (A) Trajectories of markers along the body during subsurface movement in wet media. (B) Angle of excursion of the head was calculated by comparing the low pass time-filtered snout positions to the maximum snout positions (i.e. angle of excursion would be measured from maximum excursion at  $t_1$  and  $t_2$  to the filtered position, see text for details). (C) The average maximum angle of excursion during movement in dry media is greater than in wet media.

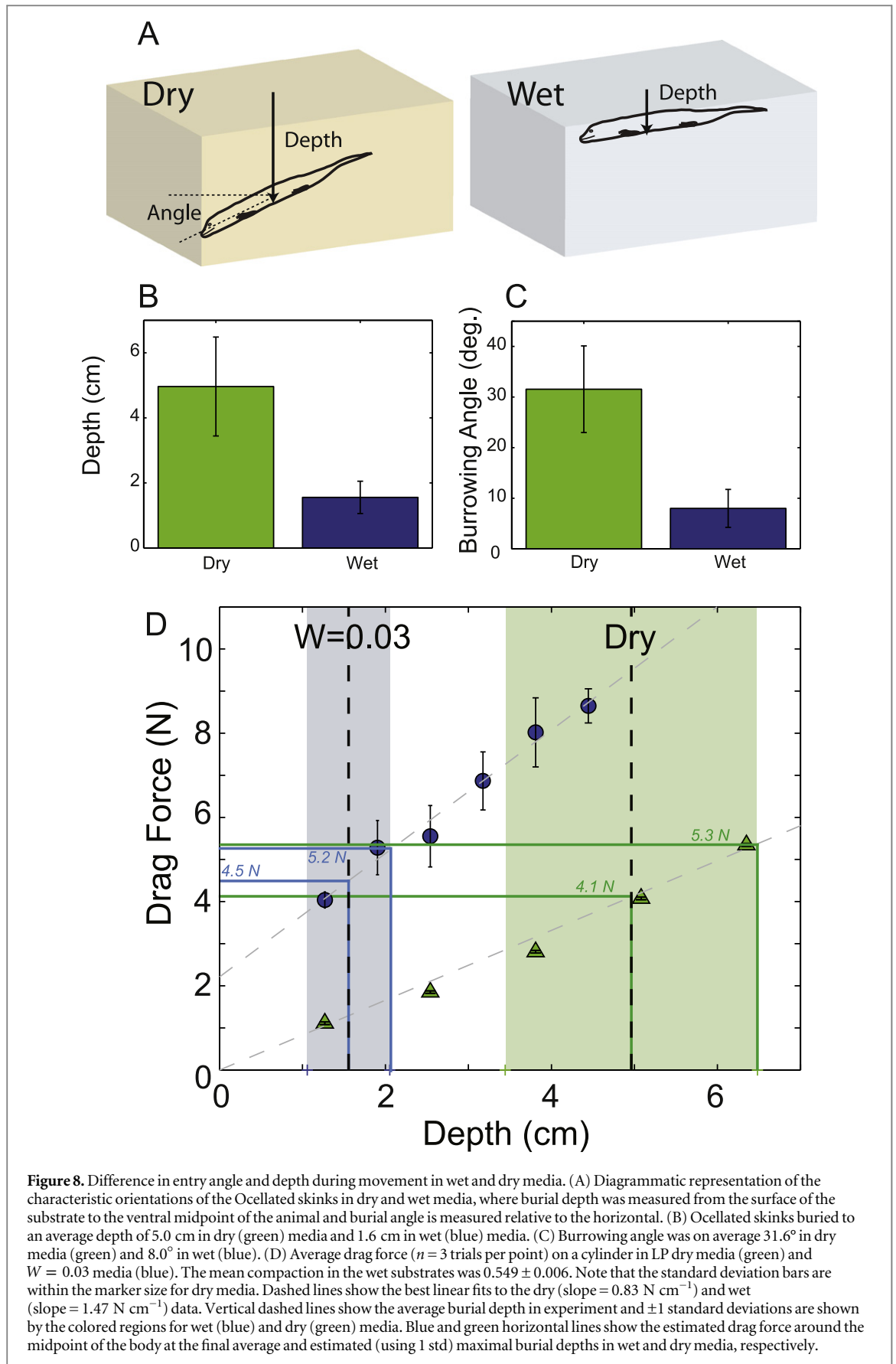
known to lead to inaccuracies in RFT in larger particles [15]) to allow confident application of RFT to such locomotor modes. In slightly wet GM like that studied here, we are not aware of similarly predictive models; development of a theoretical framework to account for resistive forces on intruders (broadening the drag measurements presented here) will be critical to explain the biological and physical observations.

#### 4.3. Burial behavior

The use of a homogenous wet GM preparation with controllable compaction allowed us to discover that Ocellated skinks bury into ground using periodic body bending movements, the forelimb on the convex side, and head oscillation. Although burial speeds are much slower than some specialized burrowers like the sandfish ( $\approx 0.5$  s for the sandfish [44] compared to 20–30 s for the Ocellated skink) the general burial strategy enabled the Ocellated skink to burrow into both wet and dry media preparations. While the sandfish burial and swimming strategy is effective in dry media, sandfish in captivity either avoid wet media (as in nature) or use a limbed digging strategy to displace the wet sand (from personal observations). This may indicate that in wet sand the sandfish swimming strategy is ineffective. We expect that this burial capability is vital for the Ocellated skink's survival in nature, because it allows thermoregulation

and conceals the skink from other animals. Attum *et al* [40] reported that Ocellated skinks were more inclined to run toward vegetation to escape predators in the wild whereas sandfish preferred burial into GM during escape. This difference in preference may be due to Ocellated skink's inability to rapidly submerge. Also, we noticed during kinematic recordings in which the media had been disturbed and large voids were present, the Ocellated skink tended to move toward the voids during subsurface locomotion. Although this was not investigated in detail, these preliminary findings could indicate that the head oscillation may be used to sense less resistance and attract the Ocellated skink to that area. In nature, the Ocellated skinks may use existing void spaces which exist in wet substrates to decrease resistance force acting on their bodies and improve performance. The Ocellated skink more readily buries into LP wet substrate than CP which may be due to the higher resistance forces in CP media. This may also indicate that in nature, Ocellated skinks preferentially bury into looser substrates.

This study has revealed an interesting pattern of subsurface locomotion which is different from the sandfish lizard. The Ocellated skink uses a start-stop motion, head oscillations, and forelimbs to move subsurface with low slip. The function of the head oscillation is still unknown. The head oscillation could serve



as (1) a force sensing mechanism (as described above) to steer motion toward low resistance regions, (2) a propulsion mechanism in which to push against the surrounding substrate, and or (3) a force reduction

mechanism to 'crack' GM and reduce resistance to intrusion similar to the activity of the annelid worm *Nereis virens* which burrows into mud by extending cracks [45].

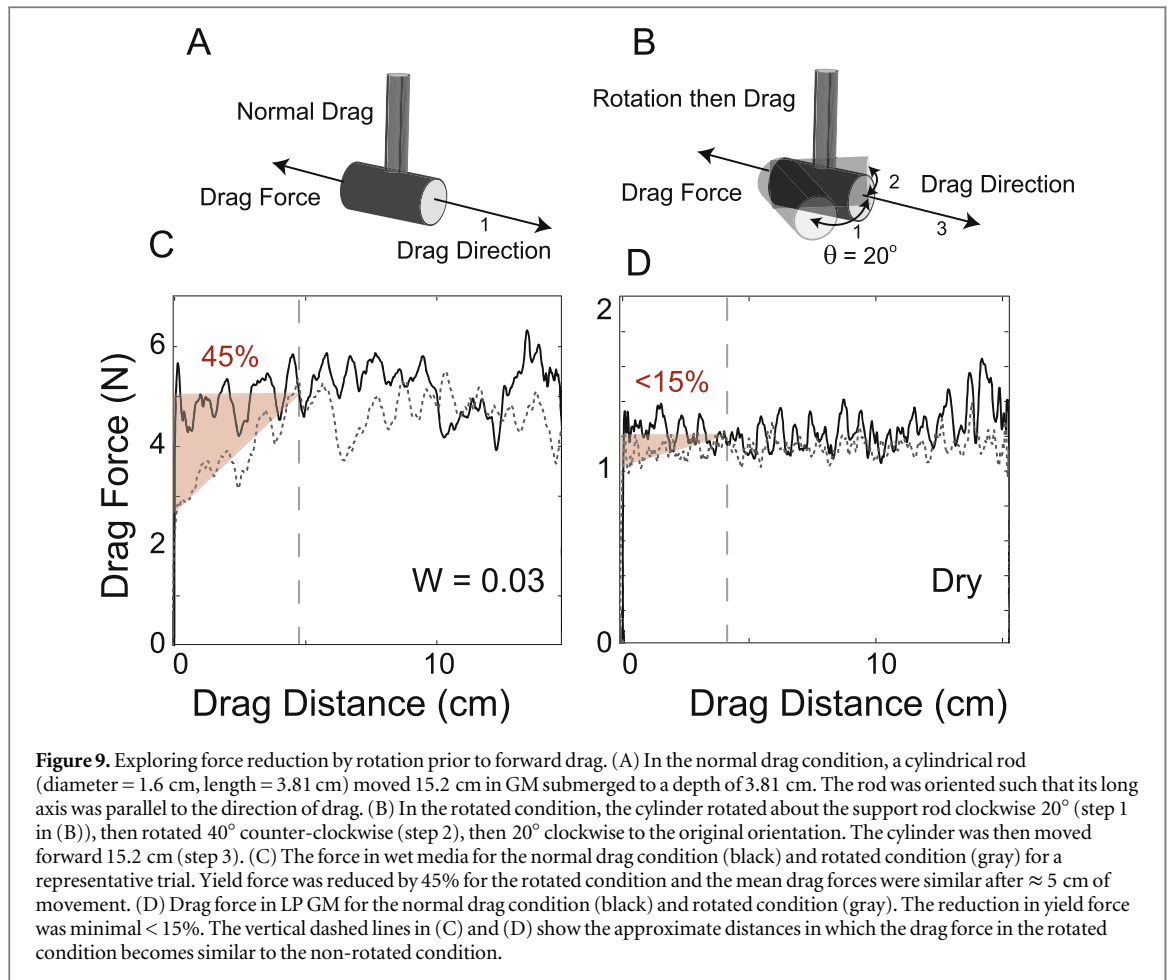


**Figure 9.** Exploring force reduction by rotation prior to forward drag. (A) In the normal drag condition, a cylindrical rod (diameter = 1.6 cm, length = 3.81 cm) moved 15.2 cm in GM submerged to a depth of 3.81 cm. The rod was oriented such that its long axis was parallel to the direction of drag. (B) In the rotated condition, the cylinder rotated about the support rod clockwise  $20^\circ$  (step 1 in (B)), then rotated  $40^\circ$  counter-clockwise (step 2), then  $20^\circ$  clockwise to the original orientation. The cylinder was then moved forward 15.2 cm (step 3). (C) The force in wet media for the normal drag condition (black) and rotated condition (gray) for a representative trial. Yield force was reduced by 45% for the rotated condition and the mean drag forces were similar after  $\approx 5$  cm of movement. (D) Drag force in LP GM for the normal drag condition (black) and rotated condition (gray). The reduction in yield force was minimal  $< 15\%$ . The vertical dashed lines in (C) and (D) show the approximate distances in which the drag force in the rotated condition becomes similar to the non-rotated condition.

To investigate whether the head oscillation could reduce resistance force during forward progression, we performed a simple experiment in which we submerged a cylindrical intruder into GM and rotated the intruder by  $+20^\circ$  and  $-20^\circ$  prior to dragging it through the granular substrate (see figure 9(B);  $n = 3$  trials). In these experiments, the rod started and moved forward with its long axis oriented parallel to the direction of movement to more closely resemble the movement of a head, although we note that both the shape and movement pattern were not intended to exactly replicate that of the Ocellated skink's movement. We found that in wet media, a rotation before drag reduced the yield force by  $\approx 45\%$  at the initial drag instant (figure 9(C)) in comparison to drag without the rotation (figures 9(A) and (C)) and approached the non-rotation drag force with increasing drag distance. After 5 cm of horizontal movement, the forces in the rotated condition matched the forces in the non-rotated condition. In dry media, the forces were similar throughout the entire horizontal drag in both conditions, indicating that the rotation was not advantageous. Unlike these simple experiments, the head oscillation in the Ocellated skink occurs *during* forward locomotion. While the oscillation could still act to reduce forces in wet media prior to the next movement, a more intriguing possibility is that the head could help to pull the animal forward. Future

computational and theoretical modeling work will be critical to reveal the purpose of the head oscillation during forward motion. It is interesting to note that the maximum head angle of excursion is higher in dry media compared to wet (even though there is little force reduction in a dry substrate, figure 9(D)). We attribute the higher angle to the lower resistance force in dry media. This may imply that the kinematic pattern is an open loop strategy in which the animal generates a constant torque at the head and kinematics change based on substrate resistance.

Ocellated skinks possess elongated bodies and reduced limbs in comparison to the sandfish. The forelimb movement on the convex side of the body reveals that limbs aid in propulsion subsurface. We received one animal that was missing nearly all of one of its forelimbs. In subsurface movement tests in dry GM (poppy seeds) we found that the animal was still able to move forward when the side with the missing limb was convex (i.e. no limb movements occurred during this period). The animal was able to move forward using only head oscillation and undulatory body motion. This may indicate that although these limbs aid in forward propulsion, head oscillation and body bending are sufficient to produce forward thrust subsurface. More rigorous experiments which constrain limbs during subsurface locomotion in dry and wet substrates are needed to further investigate the role of limbs.

#### 4.4. Burial limited by resistive force

During burial, the Ocellated skink employed a locomotion strategy in which cyclic body bending was used to enter the substrate, a strategy that enabled burial into both wet and dry substrates. However, the Ocellated skink remained near the surface of the substrate during burial into LP wet media. We attribute the lower angle and burial depth to the higher resistance forces in wet GM (figure 8(D)). Empirically measured resistance forces on a cylindrical intruder were used to estimate the forces on the skink's body at varying depths. At the Ocellated skink's final burial depth (defined as the depth of the ventral midpoint) resistance forces were 4.5 N in wet media and 4.1 N in dry media; at the burial depth extremes (+1 standard deviation) resistance forces were identical: 5.2 N in both wet and dry media. To estimate the peak forces on the animal (at the head), using the average body length and average angle of entry in wet and dry media, we calculated the depth of submersion of the head in wet and dry media and forces near the snout (as measured in rod drag experiments). In wet media, the resistance forces were lower (on average 6.7 N) than the resistance forces at the final calculated snout depth in dry media (on average 8.8 N). These measurements allow us to estimate that the Ocellated skink is capable of generating forces that are 40 times greater than its body weight, well within the range expected from animals of its size [46].

The arguments above thus indicate that the Ocellated skink is limited in its burial by the inability of its trunk (and possibly limb) muscles to conquer the basic resistive properties of the GM (with possible reduction in drag through head oscillation). It is an interesting question for further research to determine if similar limits to burial performance are seen in limbed and limbless squamates with similar body plans to the Ocellated skink (e.g. see examples in [4]). In fact, other (non-squamate) animals have evolved mechanisms to bury to depths within substrates in which resistance forces are clearly greater than forces the animal can generate; such methods include crack propagation by the annelid worm *Nereis virens* [45], fluidization and anchor method used by the Atlantic razor clam (*Ensis directus*) [25], and substrate ingestion by the earthworm (*Aporrectodea rosea*) [47]. Regarding the latter, the razor clam can produce  $\approx 10$  N of force [48] to pull itself into saturated GM which should only allow burial into a few centimeters in saturated GM; however, this animal can submerge to depths greater than 70 cm [25]. Winter *et al* [25] found that its unique valve movements fluidize the surrounding media allowing it to bury deeply while reducing the energy required to reach large depths. As another example, measurements on certain earthworms (*Aporrectodea rosea*) revealed these animals can generate a maximum force of  $\approx 3$  N using longitudinal muscles in any one segment [47], but can submerge deep within the ground ( $\approx 50$ cm [49]). To cope with

larger forces at larger depths or in compacted soils, earthworms may switch burial strategy and ingest soil to move through the medium.

## 5. Conclusions

In conclusion, we have developed a new technique to create relatively large controlled preparations of wet granular media. We used this to make the first measurements of the movement pattern of a generalist lizard burying within such substrates. The ability to control properties and generate repeatable states that were homogeneous allowed us to monitor the burial process. The Ocellated skink's movement pattern differed from the sand-specialist sandfish lizard (the only other lizard studied at this level of detail) in dry granular media (the only substrate in which the sandfish rapidly buries). And while for the Ocellated skink there were some differences in burial kinematics (e.g. head oscillation amplitude, speed, and burial entry angle) between dry and wet media, the same general locomotion strategy was employed in both conditions. We therefore hypothesize that the Ocellated skink uses a similar kinematic burial pattern, or 'template' (see [50] which defines a template as a target of neuromechanical control). In this case, resistive force properties of the substrate lead to differences in burial depth. To test for a template, future studies could perform electromyography as the animal is subjected to different substrate conditions; this approach was used in studies of a template for rapid burial in dry GM [3, 51].

However, our previous discoveries of templates in dry sand-swimming were only made possible by models of intrusion and drag in GM, which unlike true fluids, have no validated equations of motion that describe all scenarios. In those studies RFT (see for example [52]) and multi-particle discrete element method simulations (see for example [15]) revealed that by following a template, the sandfish could maximize swimming speed and minimize energy use [4, 16]. Therefore we argue that better models of wet GM during intrusion are needed to aid in modeling the locomotion of the vast diversity of animals that bury. Perhaps the approach using soil mechanics [25] could be of use to develop a more general 'terradynamics' (see [14] for discussion). Our sieving preparation technique should be useful in constructing models of intrusion: the homogeneity and repeatability will aid in direct comparison with computational and theoretical models which can be used to generate hypotheses and increase understanding of biological principles.

## Acknowledgments

We thank Tamunodiepriye George who began the kinematic work with the Ocellated skinks, Kevin Daffon for assistance with investigation of techniques

to prepare repeatable wet granular states, and Andras Karsai for his help in data analysis. We also thank Feifei Qian and Kaitlin Judy for assistance in collecting preliminary wet granular media force data. This work was supported by The Burroughs Wellcome Fund Career Award at the Scientific Interface, NSF Physics of Living Systems grants PHY-0749991 and PHY-1150760, Army Research Office Grant No. W911NF-11-1-0514, and the Army Research Laboratory (ARL) Micro Autonomous Systems and Technology (MAST) Collaborative Technology Alliance (CTA) under cooperative agreement number W911NF-08-2-0004.

## References

- [1] Nedderman R 1992 *Statics and Kinematics of Granular Materials* (Cambridge: Cambridge University Press)
- [2] Maladen R D, Ding Y, Li C and Goldman D I 2009 Undulatory swimming in sand: subsurface locomotion of the sandfish lizard *Science* **325** 314–8
- [3] Sharpe S S, Ding Y and Goldman D I 2012 Environmental interaction influences muscle activation strategy during sand-swimming in the sandfish lizard *Scincus scincus* *J. Exp. Biol.* **216** 260–74
- [4] Sharpe S S, Koehler S A, Kuckuk R M, Serrano M, Vela P A, Mendelson J III and Goldman D I 2015 Locomotor benefits of being a slender and slick sand-swimmer *J. Exp. Biol.* **218** 440–50
- [5] Marvi H et al 2014 Sidewinding with minimal slip: snake and robot ascent of sandy slopes *Science* **346** 224–9
- [6] Mazouchova N, Gravish N, Savu A and Goldman D I 2010 Utilization of granular solidification during terrestrial locomotion of hatchling sea turtles *Biol. Lett.* **6** 398–401
- [7] Li C, Hsieh S T and Goldman D I 2012 Multi-functional foot use during running in the zebra-tailed lizard (*Callisaurus draconoides*) *J. Exp. Biol.* **215** 3293–308
- [8] Irschick D J and Jayne B C 1999 A field study of the effects of incline on the escape locomotion of a bipedal lizard, *Callisaurus draconoides* *Physiol. Biochem. Zoology* **72** 44–56
- [9] Korff W L and McHenry M J 2011 Environmental differences in substrate mechanics do not affect sprinting performance in sand lizards (*Uma scoparia* and *Callisaurus draconoides*) *J. Exp. Biol.* **214** 122–30
- [10] Maladen R D, Ding Y, Umbanhowar P B, Kamor A and Goldman D I 2011 Mechanical models of sandfish locomotion reveal principles of high performance subsurface sand-swimming *J. R. Soc. Interface* **8** 1332–45
- [11] Maladen R D, Ding Y, Umbanhowar P B and Goldman D I 2011 Undulatory swimming in sand: experimental and simulation studies of a robotic sandfish *Int. J. Robot. Res.* **30** 793–805
- [12] Maladen R D, Umbanhowar P B, Ding Y, Masse A and Goldman D I 2011 Granular lift forces predict vertical motion of a sand-swimming robot *IEEE Int. Conf. on Robotics and Automation (ICRA)* pp 1398–403
- [13] Li C, Umbanhowar P B, Komsuoglu H, Koditschek D E and Goldman D I 2009 Sensitive dependence of the motion of a legged robot on granular media *Proc. Natl Acad. Sci.* **106** 3029
- [14] Li C, Zhang T and Goldman D I 2013 A terradynamics of legged locomotion on granular media *Science* **339** 1408–12
- [15] Ding Y, Sharpe S S, Masse A and Goldman D I 2012 Mechanics of undulatory swimming in a frictional fluid *PLoS Comput. Biol.* **8** e1002810
- [16] Goldman D I 2014 Colloquium: biophysical principles of undulatory self-propulsion in granular media *Rev. Mod. Phys.* **86** 943
- [17] European-Environmental-Agency 2012 Global surface soil moisture content based on remote sensing data (available: <http://eea.europa.eu/data-and-maps/>)
- [18] Fournier Z et al 2005 Mechanical properties of wet granular materials *J. Phys.: Condens. Matter.* **17** S477
- [19] Mitarai N and Nori F 2006 Wet granular materials *Adv. Phys.* **55** 1–45
- [20] Herminghaus S 2005 Dynamics of wet granular matter *Adv. Phys.* **54** 221–61
- [21] Jung S 2010 *Caenorhabditis elegans* swimming in a saturated particulate system *Phys. Fluids* **22** 031903
- [22] Trueman E R 1970 The mechanism of burrowing of the mole crab, *emerita* *J. Exp. Biol.* **53** 701–10
- [23] Juarez G, Lu K, Sznitman J and Arratia P E 2010 Motility of small nematodes in wet granular media *Europhys. Lett.* **92** 44002
- [24] Ducey P K, Formanowicz D R Jr, Boyet L, Mailloux J and Nussbaum R A 1993 Experimental examination of burrowing behavior in caecilians (Amphibia: Gymnophiona): effects of soil compaction on burrowing ability of four species *Herpetologica* **49** 450–7
- [25] Winter A G, Deits R L H and Hosoi A E 2012 Localized fluidization burrowing mechanics of *Ensis directus* *J. Exp. Biol.* **215** 2072–80
- [26] Gidmark N J, Strother J A, Horton J M, Summers A P and Brainerd E L 2011 Locomotory transition from water to sand and its effects on undulatory kinematics in sand lances (ammodytidae) *J. Exp. Biol.* **214** 657–64
- [27] Kornilios P, Kyriazi P, Poulakakis N, Kumlutaş Y, Ilgaz Ç, Mylonas M and Lymberakis P 2010 Phylogeography of the ocellated skink *Chalcides ocellatus* (squamata, scincidae), with the use of mtDNA sequences: a hitch-hikers guide to the Mediterranean *Mol. Phylogenetics and Evol.* **54** 445–56
- [28] Scheel M, Seemann R, Brinkmann M, Di Michiel M, Sheppard A, Breidenbach B and Herminghaus S 2008 Morphological clues to wet granular pile stability *Nat. Mater.* **7** 189–93
- [29] Richefeu V, El Youssoufi M S and Radjai F 2006 Shear strength properties of wet granular materials *Phys. Rev. E* **73** 051304
- [30] Dickinson W W and Ward J D 1994 Low depositional porosity in eolian sands and sandstones, Namib desert *J. Sedimentary Res.* **64** 226–32
- [31] Gravish N, Umbanhowar P B and Goldman D I 2010 Force and flow transition in plowed granular media *Phys. Rev. Lett.* **105** 128301
- [32] Marston J O, Vakarelski I U and Thoroddsen S T 2012 Sphere impact and penetration into wet sand *Phys. Rev. E* **86** 020301
- [33] Jackson S J, Whyte M A and Romano M 2009 Laboratory-controlled simulations of dinosaur footprints in sand: a key to understanding vertebrate track formation and preservation *Palaio* **24** 222–38
- [34] Schubert H, Herrmann W and Rumpf H 1975 Deformation behaviour of agglomerates under tensile stress *Powder Technol.* **11** 121–31
- [35] Vandewalle N, Lumay G, Ludewig F and Fiscina J E 2012 How relative humidity affects random packing experiments *Phys. Rev. E* **85** 031309
- [36] Gioia G, Cuitiño A M, Zheng S and Uribe T 2002 Two-phase densification of cohesive granular aggregates *Phys. Rev. Lett.* **88** 204302
- [37] Fiscina J E, Lumay G, Ludewig F and Vandewalle N 2010 Compaction dynamics of wet granular assemblies *Phys. Rev. Lett.* **105** 048001
- [38] Carranza S, Arnold E, Geniez P, Roca J and Mateo J 2008 Radiation, multiple dispersal and parallelism in the skinks, chalcides and sphepops (squamata: Scincidae), with comments on scincus and scincopus and the age of the Sahara desert *Mol. Phylogenetics and Evol.* **46** 1071–94
- [39] Greer A E, Caputo V, Lanza B and Palmieri R 1998 Observations on limb reduction in the scincid lizard genus *Chalcides* *J. Herpetology* **244**–52
- [40] Attum O, Eason P and Cobbs G 2007 Morphology, niche segregation, and escape tactics in a sand dune lizard community *J. Arid Environ.* **68** 564–73
- [41] Albert R, Pfeifer M A, Barbási A L and Schiffer P 1999 Slow drag in a granular medium *Phys. Rev. Lett.* **82** 205

- [42] Hu D L, Nirody J, Scott T and Shelley M J 2009 The mechanics of slithering locomotion *Proc. Natl Acad. Sci.* **106** 10081–5
- [43] Comanns P, Effertz C, Hischen F, Staudt K, Böhme W and Baumgartner W 2011 Moisture harvesting and water transport through specialized micro-structures on the integument of lizards *Beilstein J. Nanotechnology* **2** 204–14
- [44] Sharpe S 2013 Control of burial and subsurface locomotion in particulate substrates *PhD Dissertation* Georgia Institute of Technology
- [45] Dorgan K M, Jumars P A, Johnson B, Boudreau B P and Landis E 2005 Burrowing mechanics: burrow extension by crack propagation *Nature* **433** 475
- [46] Alexander R M 1985 The maximum forces exerted by animals *J. Exp. Biol.* **115** 231–8
- [47] McKenzie B and Dexter A 1988 Radial pressures generated by the earthworm *Aporrectodea rosea* *Biol. Fertility Soils* **5** 328–32
- [48] Trueman E R 1967 The dynamics of burrowing in *Ensis* (bivalvia) *Proc. R. Soc. B* **166** 459–76
- [49] Joschko M, Diestel H and Larink O 1989 Assessment of earthworm burrowing efficiency in compacted soil with a combination of morphological and soil physical measurements *Biol. Fertility Soils* **8** 191–6
- [50] Full R J and Koditschek D E 1999 Templates and anchors: neuromechanical hypotheses of legged locomotion on land *J. Exp. Biol.* **202** 3325–32
- [51] Ding Y, Sharpe S S, Wiesenfeld K and Goldman D I 2013 Emergence of the advancing neuromechanical phase in a resistive force dominated medium *Proc. Natl Acad. Sci.* **110** 10123–8
- [52] Zhang T and Goldman D I 2014 The effectiveness of resistive force theory in granular locomotion *Phys. Fluids* **26** 101308